

Calculation of electron emission from a gated single nanowire

Da Lei, Weibiao Wang, Leyong Zeng, and Jingqiu Liang

Citation: *J. Vac. Sci. Technol. B* **27**, 2217 (2009); doi: 10.1116/1.3205005

View online: <http://dx.doi.org/10.1116/1.3205005>

View Table of Contents: <http://avspublications.org/resource/1/JVTBD9/v27/i5>

Published by the AVS: Science & Technology of Materials, Interfaces, and Processing

Related Articles

GaN surface electron field emission efficiency enhancement by low-energy photon illumination
J. Vac. Sci. Technol. B **30**, 022206 (2012)

First-principles study of field-emission from carbon nanotubes in the presence of methane
J. Vac. Sci. Technol. B **30**, 021803 (2012)

Effect of ballast-resistor and field-screening on electron-emission from nanodiamond emitters fabricated on micropatterned silicon pillar arrays
J. Vac. Sci. Technol. B **30**, 012201 (2012)

Characteristics of PMN-PZT ferroelectric electron emitters with three-dimensional emission sites formed by chemical etching
J. Vac. Sci. Technol. B **29**, 032210 (2011)

Stabilized electron emission from silicon coated carbon nanotubes for a high-performance electron source
J. Vac. Sci. Technol. B **29**, 02B120 (2011)

Additional information on *J. Vac. Sci. Technol. B*

Journal Homepage: <http://avspublications.org/jvstb>

Journal Information: http://avspublications.org/jvstb/about/about_the_journal

Top downloads: http://avspublications.org/jvstb/top_20_most_downloaded

Information for Authors: http://avspublications.org/jvstb/authors/information_for_contributors

ADVERTISEMENT

AVS 59th International Symposium & Exhibition
October 28–November 2, 2012 • Tampa, Florida

 212-248-0200
avsnyc@avs.org
www.avs.org



DIVISION/GROUP PROGRAMS:

- Advanced Surface Engineering
- Applied Surface Science
- Biomaterial Interfaces
- Electronic Materials & Processing
- Magnetic Interfaces & Nanostructures
- Manufacturing Science & Technology
- MEMS & NEMS
- Nanometer-Scale Science & Technology
- Plasma Science & Technology
- Surface Science
- Thin Film
- Vacuum Technology

FOCUS TOPICS:

- Actinides & Rare Earths
- Biofilms & Biofouling: Marine, Medical, Energy
- Biointerphases
- Electron Transport at the Nanoscale
- Energy Frontiers
- Exhibitor Technology Spotlight
- Graphene & Related Materials
- Helium Ion Microscopy
- *InSitu* Microscopy & Spectroscopy
- Nanomanufacturing
- Oxide Heterostructures-Interface Form & Function
- Scanning Probe Microscopy
- Spectroscopic Ellipsometry
- Transparent Conductors & Printable Electronics
- Tribology

Calculation of electron emission from a gated single nanowire

Da Lei

Laboratory of Excited-State Processes, Changchun Institute of Optics, Fine Mechanics and Physics, Chinese Academy of Sciences, Changchun 130033, China and Graduate School of Chinese Academy of Sciences, Beijing 100039, China

Weibiao Wang^{a)}

Laboratory of Excited-State Processes, Changchun Institute of Optics, Fine Mechanics and Physics, Chinese Academy of Sciences, Changchun 130033, China

Leyong Zeng

Laboratory of Excited-State Processes, Changchun Institute of Optics, Fine Mechanics and Physics, Chinese Academy of Sciences, Changchun 130033, China and Graduate School of Chinese Academy of Sciences, Beijing 100039, China

Jingqiu Liang

State Key Laboratory of Applied Optics, Changchun Institute of Optics, Fine Mechanics and Physics, Chinese Academy of Sciences, Changchun 130033, China

(Received 22 August 2008; accepted 12 July 2009; published 15 September 2009)

The field-enhancement factor β on an individual nanowire with flattop was calculated analytically by the electrostatic method in a gated structure. To evaluate the influences of the geometrical parameters—including the gate-hole radius R , nanowire radius r_0 , nanowire length L , and gate-anode distance d_2 for β —the authors proposed an ideal model of the gated single nanowire ($L < d_1$), where d_1 is the gate-cathode space. The calculation results showed that β decreases rapidly with both R and r_0 and eventually saturates to a fixed value if R tends to infinity. It increases almost linearly with an increase in the nanowire height. When d_2 is not much larger than d_1 and R , β decreases slightly as d_2 increases, but the effect of the gate-anode distance on β can be ignored if d_2 is infinite. These results provide useful information on fabricating and designing gated nanowire cold cathodes for field-emission display panels and other nanoscale triodes. © 2009 American Vacuum Society. [DOI: 10.1116/1.3205005]

I. INTRODUCTION

Nanowires are one of the most exciting discoveries in nanoscale physics.^{1,2} They are one of best electron-emitting materials available because of their remarkable field-emission properties for application to vacuum microelectronic devices.^{3–5} The unique structure of nanowires can generate a large electric-field enhancement. This leads to a greater local field at the top of nanowires, and the emission electrons can penetrate the potential barrier into the vacuum using the tunneling effect.^{6,7} A higher current density occurs at a low external electric field. Therefore, nanowires are considered ideal candidates for next-generation field emitters for flat-panel displays, field-emission electron sources, and microwave power amplifiers.^{8–10}

Studies have shown that many parameters, including the aspect ratio of nanowires, anode-cathode distance, and interwire distance, can influence the field-emission properties of the nanowires.^{11–18} In particular, the gate-hole radius, gate-anode distance, and gate voltage can affect the emission properties of the nanowires in triodes or gated devices.^{19–25} The field-enhancement factor is an important factor that in-

dicates the field-emission properties of field-emission cold cathode devices. It is generally related linearly to the aspect ratio of nanoemitters in diode models. At present, such studies have mainly concentrated on diode structures. Wang and co-workers,^{16,17} using the image method and floated-sphere model, explained the influence of the intertube distance and anode-cathode distance for the field-enhancement factor on a planar cathode surface.

Many experimental and theoretical analyses have proven^{22–25} that the electric field at the nanoemitter top surface is a linear equation of the anode V_a and gate V_g voltages in the triodes. Nicolaescu and co-workers^{22,24,25} reported the relationship between the field correlation factors and the geometrical parameters of the nanotriode using the numerical simulation method and SIMION 3D 7.0. The variation behaviors of the field correlation factors for the gate-hole radius, emitter height, and top radius of the nanowire were developed. The computer simulation and numerical calculation methods (for solving Laplace's equation) were successful in calculating the field distribution at the top of the nanowire and the field-enhancement factor in various cases. However, there is a need for model systems that can be solved analytically, from which the variation in the enhancement factor for various parameters can be easily determined.

In this article, the actual fields at the top surface of the gated nanowire and the enhancement factor of the apex were

^{a)}Author to whom correspondence should be addressed; also at Laboratory of Excited-State Processes, Changchun Institute of Optics, Fine Mechanics and Physics, Chinese Academy of Sciences, Changchun 130033, China; electronic mail: wangwb@126.com

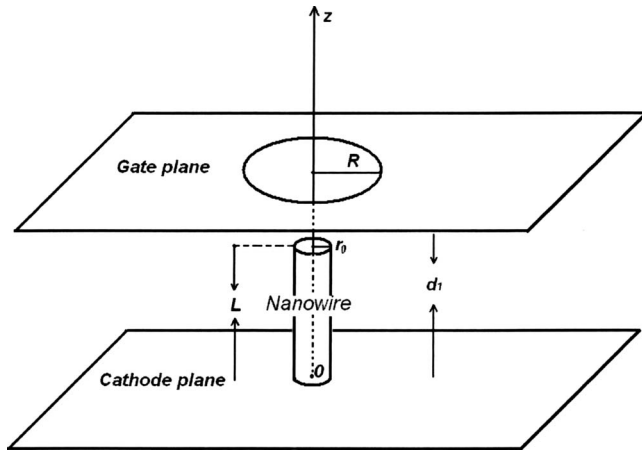


FIG. 1. Model of the gated nanowire.

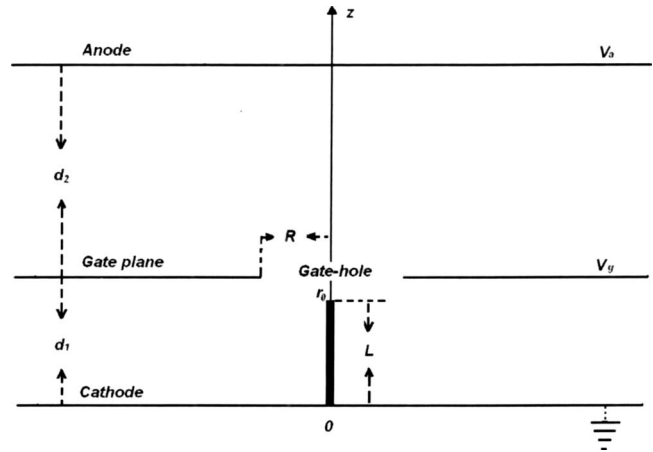


FIG. 2. Calculation model of the gated nanowire.

calculated for the case where the nanowire is lower than that of the gate plane. The field-enhancement factor is expressed by $\beta = \lambda_a + \gamma_g$, where $\gamma_g = \eta(d_2 + d_1) \cdot V_g / V_a$, $\lambda_a = \lambda(d_2 + d_1)$, λ and η are functions of the geometrical parameters, and V_g and V_a are the gate and anode voltages, respectively. Finally, we investigated the behavior of the field-enhancement factor versus gate-hole radius, nanowire radius, nanowire length, and gate-anode distance. The variation behavior of field-enhancement factor for geometrical parameters agrees with the theoretical results.^{24,25} These results provide useful information on fabricating and designing gated nanowire cold cathodes for field-emission display panels and other nanoscale triodes.

II. MODELING AND CALCULATIONS

A. Model

The model system of the gated single-nanowire cold cathode is described as follows. One of the nanowire with a flat top is regarded as the emitter of the cold cathode, which is considered a conductive cylinder with radius r_0 , placed vertically on an infinite cathode plane under the center of the gate circular hole with radius R (several micrometers), as shown in Fig. 1. Another infinite thin plane, which is taken as the gate electrode with a potential of V_g , where the thickness of plane can be neglected, is parallel to the cathode plane and the spacing to the cathode is d_1 (several micrometers). The potential of the nanowire surface is maintained at zero, which is equal to the cathode potential.

In the two-dimensional model, an additional anode electrode with V_a potential is introduced and is parallel to the gate electrode, where d_2 is the space from the gate electrode, as shown in Fig. 2. To simulate the field emission from the gated nanowire, we assume that the height of the nanowire is L , and the space-charge effects and edge effects of the devices are neglected.

B. Field calculations near the nanowire

The cylindrical coordinate system was used, and the origin was selected at the intersection point of the cathode plane

and tube axis. Because space-charge effects are ignored, the potential distribution near the nanowire in the triode satisfies Laplace's equation,

$$\nabla^2 \Phi(z, r, \varphi) = 0. \tag{1}$$

The boundary conditions of the potential distribution are as follows: $\Phi|_{z=0} = 0$, $(\partial\Phi/\partial r)|_{r=d_1+d_2} = 0$, $\Phi|_{z=d_1+d_2} = V_a$, $\Phi|_{z=d_1} = V_g$, and $\Phi|_{r=r_0} = 0$ in the range of $0 \leq z \leq L$.

Solutions for potential will be obtained for the two regions, $z \leq L$ and $z \geq L$, and will be matched at $Z=L$, $r=R$. Thus, the solutions of Eq. (1) can be obtained by separation of variables when $k=0$ and $k>0$, respectively,

$$\Phi(z, r) = (az + b)(A \ln r + B) \quad (k = 0), \tag{2}$$

$$\Phi(z, r) = [a' \exp(kz) + b' \exp(-kz)][A' J_0(kr) + B' N_0(kr)] \quad (k > 0), \tag{3}$$

where $k, a, b, A, B, a', b', A',$ and B' are constants and $J_0(kr)$ and $N_0(kr)$ are Bessel and Neumann functions of the order of zero, respectively.

The function $\Phi(z, r)$ must be of finite value in the region $L \leq z \leq (d_1 + d_2)$ because the potentials are finite in our model. However, as r tends to zero, then the two terms $\ln(r)$ and $N'_0(kr)$ above are diverge as $\lim_{r \rightarrow 0} \ln(r) \rightarrow -\infty$ and $\lim_{r \rightarrow 0} N_0(kr) \rightarrow -\infty$. Hence, the potential distribution will only be finite when $A=0, B'=0$ in Eqs. (2) and (3), which become

$$\Phi = az + b, \tag{4}$$

$$\Phi(z, r) = A'[a' \exp(kz) + b' \exp(-kz)]J_0(kr). \tag{5}$$

Considering the boundary conditions $(\partial\Phi/\partial r)|_{r=d_1+d_2} = 0$ and $\Phi|_{z=d_1+d_2} = V_a$, the potential distribution over the top of the nanowire may be expressed by

$$\Phi(z, r) = V_a - a(d_1 + d_2 - z) + \sum_k C_k \exp(-kz) \times \{1 - \exp[-2k(d_1 + d_2 - z)]\}J_0(kr), \tag{6}$$

where C_k is constant. This solution will be approximated by

using only one value of k . This value of k is defined later by Eq. (14).

The local electric fields are only calculated near the surface of the nanowire (in the region $r \leq R$) in our work. Therefore, it is not necessary to consider the potential distribution in the region $r > R$ when the gate-hole radius is much larger than the nanowire radii r_0 . According to the properties of Bessel functions and the boundary conditions $\Phi|_{z=d_1}^{r=R} = V_g$ and $\Phi|_{z=L}^{r=0} = 0$, the approximate solution of the electric potential over the top of the nanowire in the region $r \leq R$ is

$$\Phi(z, r) = V_a - a(d_1 + d_2 - z) + C \frac{\exp(-k_1 z) \{1 - \exp[-2k_1(d_1 + d_2 - z)]\}}{\exp(-k_1 L) \{1 - \exp[-2k_1(d_1 + d_2 - L)]\}} J_0(k_1 r), \quad (7)$$

where k_1 , a , and C are constants and a and C are determined by the following equations:

$$a \approx \frac{V_a \exp[-k_1(d_1 - L)] J_0(k_1 R) - (V_a - V_g) J_0(k_1 r_0)}{(d_1 + d_2 - L) \exp[-k_1(d_1 - L)] J_0(k_1 R) - d_2 J_0(k_1 r_0)},$$

$$C = \frac{[(d_1 + d_2 - L) V_g - (d_1 - L) V_a]}{(d_1 + d_2 - L) \exp[-k_1(d_1 - L)] J_0(k_1 R) - d_2 J_0(k_1 r_0)},$$

respectively. In obtaining these relations, $\exp(-2k_1 d_2)$ has been ignored in comparison with 1.

Hence, the fields over the top of the nanowire can be expressed by

$$E_{tr} = -k_1 C \frac{\exp(-k_1 z) \{1 - \exp[-2k_1(d_1 + d_2 - z)]\}}{\exp(-k_1 L) \{1 - \exp[-2k_1(d_1 + d_2 - L)]\}} J_1(k_1 r), \quad (8)$$

$$E_{tz} = -a + k_1 C \frac{\exp(-k_1 z) \{1 + \exp[-2k_1(d_1 + d_2 - z)]\}}{\exp(-k_1 L) \{1 - \exp[-2k_1(d_1 + d_2 - L)]\}} J_0(k_1 r). \quad (9)$$

We now consider a second solution for potential for use in the region $z \leq L$. Similarly, considering the boundary conditions $\Phi|_{z=0} = 0$ and $\Phi|_{r=r_0} = 0$ in the case of $0 \leq z \leq L$, the electric potential distribution near the outside of the nanowire can be expressed by

$$\Phi(z, r) = \sum_{i=1}^{\infty} A_i'' \left[J_0(k_i r) - \frac{J_0(k_i r_0)}{N_0(k_i r_0)} N_0(k_i r) \right] \text{sh}(k_i z), \quad (10)$$

where $A_i'' (i=1, 2, 3, \dots)$ are constants.

On the other hand, the electric potential must be a solution of Laplace's equation (1), so Eq. (10) can be rewritten as $\Phi(z, r) = \sum \Psi_1(z) \times \Psi_2(r)$, where $\Psi_1(z)$ and $\Psi_2(r)$ are functions of z and r , respectively. From Eq. (3), we can see that the function $\Psi_2(r)$ can be expressed as a linear superposition of both Bessel $J_0(k'r)$ and Neumann $N_0(k'r)$ functions in the range of $k' > 0$, i.e., $\Psi_2(r) = C'' J_0(k'r) + D N_0(k'r)$, where k' , C'' , and D are constants. Based on the boundary condition $\Phi|_{r=r_0} = 0$, the function above can be written as $\Psi_2(r)$

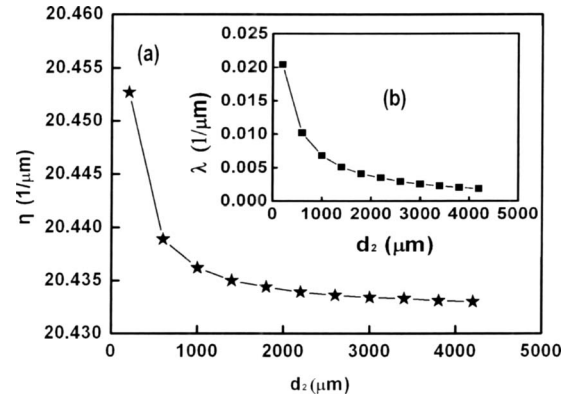


FIG. 3. Curves of the gate and anode field correlation factors η and λ for the gate-anode distance d_2 .

$= C' [J_0(k'r) - J_0(k'r_0) N_0(k'r) / N_0(k'r_0)]$. Thus, the function $\Phi(L, r)$ can be expressed by $\Phi(L, r) = U_m [J_0(k'r) - J_0(k'r_0) N_0(k'r) / N_0(k'r_0)]$ at $z=L$, $r > r_0$, where C' and U_m are coefficients. If assumed as $k' = k_1$, the following equations $A_i'' = U_m / \text{sh}(k_1 L)$, $A_i'' = 0$ ($i=2, 3, 4, \dots$) are obtained from Eq. (10), and the electric potential around the outside of the can be rewritten as

$$\Phi(z, r) = U_m \frac{\text{sh}(k_1 z)}{\text{sh}(k_1 L)} \left[J_0(k_1 r) - \frac{J_0(k_1 r_0) N_0(k_1 r)}{N_0(k_1 r_0)} \right]. \quad (11)$$

The potential and axial electric fields should be continuous at $z=L$ for $r < R$. To approximate this condition, we set Eq. (7) equal to Eq. (11) at $z=L$, $r=R$. Thus, U_m obtained from Eqs. (7) and (11) and expressions of a and C is

$$U_m = \frac{[(d_1 + d_2 - L) V_g - (d_1 - L) V_a]}{(d_1 + d_2 - L) \exp[-k_1(d_1 - L)] J_0(k_1 R) - d_2 J_0(k_1 r_0)}.$$

Hence, the following corresponding electric-field intensities near the outside of the nanowire are obtained as:

$$E_{sz} = k_1 U_m \frac{\text{ch}(k_1 z)}{\text{sh}(k_1 L)} \left[J_0(k_1 r) - \frac{J_0(k_1 r_0) N_0(k_1 r)}{N_0(k_1 r_0)} \right], \quad (12)$$

$$E_{sr} = k_1 U_m \frac{\text{sh}(k_1 z)}{\text{sh}(k_1 L)} \left[J_1(k_1 r) - \frac{J_0(k_1 r_0) N_1(k_1 r)}{N_0(k_1 r_0)} \right], \quad (13)$$

where E_{sr} and E_{sz} are the electric-field intensities in the radial and axial directions in the case of $r \geq r_0$, $0 \leq z \leq L$.

In addition, Eq. (14) can be obtained if we assume that the potentials amount to about $V_g L / d_1$ at the points of $z=L$, where $r \geq R$ because the electric field in the triode tends to a uniform field when r tends to infinity,

$$\frac{V_g L}{d_1} = U_m \left[J_0(k_1 R) - \frac{J_0(k_1 r_0) N_0(k_1 R)}{N_0(k_1 r_0)} \right]. \quad (14)$$

Thus, k_1 is determined by Eq. (14).

III. FIELD-ENHANCEMENT FACTOR

The field-enhancement factor β is defined as $\beta = E_a / E_m$,^{16,17} where E_a is the actual electric field at the

apex of the nanowire and E_m is the macroscopic applied electric field. To compute the enhancement factor, the actual electric field on the edge of the nanowire is calculated from Eqs. (9) and (13) at $r=r_0, z=L$. Thus, the actual electric field at the top edge of the nanowire can be expressed by

$$E_a = \sqrt{E_{sr}^2 + E_{rz}^2} \tag{15}$$

E_{tr} expresses only the electric field over the top of nanowire at the radial direction and is discontinuous on the flattop of the nanowire so it does not explain the part of electric field on the nanowire top edge at the radial direction as z

$=L, r=r_0$. Thus we choose to use E_{sr} as the electric field on the nanowire top edge at radial direction in Eq. (15).

According to our model, the macroscopic electric field between the anode and the cathode can be expressed as $E_m = V_a/(d_1+d_2)$ in the diode structure (without a gate electrode), which corresponds to macroscopic electric field in this study. Hence, obtained the field-enhancement factor is obtained by

$$\beta = \lambda_a + \gamma_g, \tag{16}$$

where $\lambda_a = \lambda(d_2+d_1)$, $\gamma_g = \eta(d_2+d_1) \cdot V_g/V_a$, λ and η are called the anode field correlation factor and the gate field correlation factor,^{24,25} which are determined by

$$\lambda \approx \frac{k_1(L-d_1)[J_1(k_1r_0)N_0(k_1r_0) - J_0(k_1r_0)N_1(k_1r_0)]}{\{(d_1+d_2-L)\exp[-k_1(d_1-L)]J_0(k_1R) - d_2J_0(k_1r_0)\}N_0(k_1r_0)},$$

$$\eta \approx \frac{k_1(d_1+d_2-L)[J_1(k_1r_0)N_0(k_1r_0) - J_0(k_1r_0)N_1(k_1r_0)]}{\{(d_1+d_2-L)\exp[-k_1(d_1-L)]J_0(k_1R) - d_2J_0(k_1r_0)\}N_0(k_1r_0)},$$

respectively.

IV. RESULTS AND DISCUSSION

To particularize the influences of the geometrical parameters on field-enhancement factor, the variation behaviors of the enhancement factor for d_2, L, r_0 , and R are calculated at $d_1=10 \mu\text{m}$, $V_a=2000 \text{ V}$, and $V_g=100 \text{ V}$.

The variation curves of the anode field correlation factor λ and gate field correlation factor η for the gate-anode distance are given in Figs. 3(a) and 3(b) at $r_0=10 \text{ nm}$, $L=9.8 \mu\text{m}$, and $R=3 \mu\text{m}$. We can see the anode field correlation factor and gate field correlation factor increase slowly with the decreases in the gate-anode distance when d_2 is finite and λ and η are the similar variation behaviors for

d_2 . However, the effects of d_2 on the correlation factors can be neglected when d_2 is infinite. Thus, the field-enhancement factor decreases as d_2 increases when d_2 is finite. The influence of d_2 on the β can be neglected when d_2 is infinite.

The field-enhancement factor can be expressed simply by Eq. (16) as long as the field correlation factors have been determined. The variation behavior of the enhancement factor versus L is almost linear, with a slope of $29.35/\mu\text{m}$ at $d_2=500 \mu\text{m}$, $r_0=10 \text{ nm}$, and $R=5 \mu\text{m}$, as shown in Fig. 4.

Figure 5 shows the influence of the nanowire radius on the enhancement factor at $d_2=500 \mu\text{m}$, $R=5 \mu\text{m}$, and $L=9.8 \mu\text{m}$. We can see that the enhancement factor decreases as the nanowire radius increases. The above variation behaviors are similar to the behavior of enhancement factors for

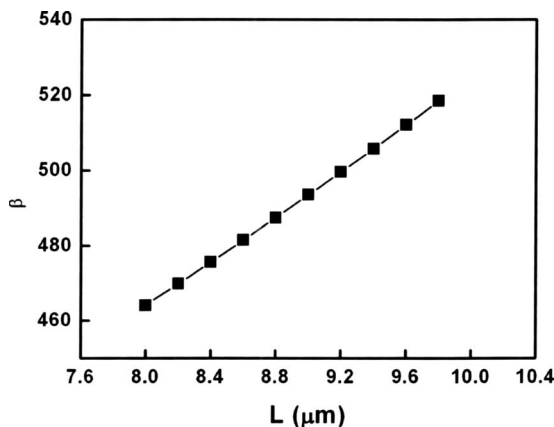


FIG. 4. Plot of the field-enhancement factor β as a function of the nanowire length L .

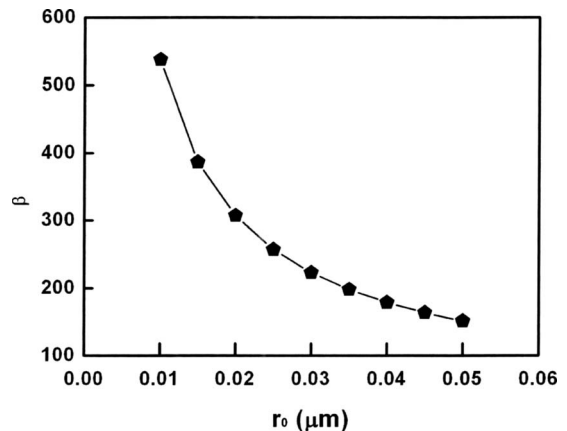


FIG. 5. Variation curve of the field-enhancement factor β for the nanowire radius r_0 .

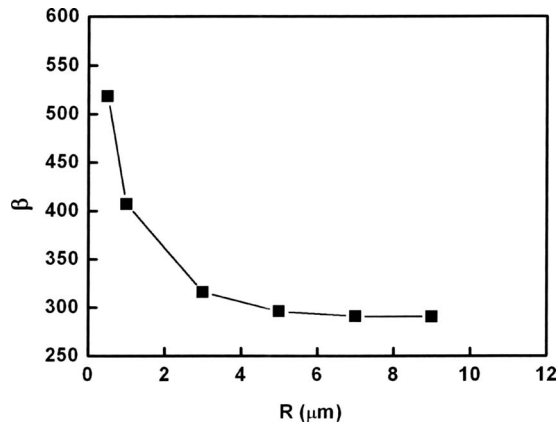


FIG. 6. Variation curve of the field-enhancement factor β vs the gate-hole radius R .

individual nanowires on the planar cathode.^{11–18} The enhancement factor as a function of the gate-hole radius at $d_2 = 500 \mu\text{m}$, $r_0 = 10 \text{ nm}$, and $L = 9.8 \mu\text{m}$ is shown in Fig. 6. We find that the enhancement factor decreases greatly as the gate-hole radius increases and tends to a fixed value if R tends to infinity. This is because the influences of the gate-hole brim for the electric field at its center are very weakly when a larger gate-hole radius. These results agree with numerical simulation results.^{24,25}

V. CONCLUSION

An ideal model, i.e., a gated single open nanowire cold cathode is proposed, and we investigated the actual electric field at the nanowire apex, field correlation factors, and enhancement factor. The calculation results agree well with experimental and theoretical results.^{19–25} Therefore, they provide useful information in fabricating and designing gated nanowire cold cathodes for field-emission display panels and other nanoscale triode devices.

ACKNOWLEDGMENT

The authors gratefully acknowledge the financial support from the National Natural Science Foundation of China (Grant Nos. 50072029 and 50572101).

¹S. Ijima, *Nature (London)* **354**, 56 (1991).

²S. Ijima and T. Ichihashi, *Nature (London)* **363**, 603 (1993).

³W. I. Milne, K. B. K. Teo, M. Chhowalla, G. A. J. Amaratunga, P. Legagneux, G. Pirio, V. T. Binh, and V. Semet, *Curr. Appl. Phys.* **2**, 509 (2002).

⁴W. Zhua, C. Bower, O. Zhou, G. Kochanski, and S. Jin, *Appl. Phys. Lett.* **75**, 873 (1999).

⁵G. Pirio, P. Legagneux, D. Pribat, K. B. K. Teo, M. Chhowalla, G. A. J. Amaratunga, and W. I. Milne, *Nanotechnology* **13**, 1 (2002).

⁶P. N. Minh, L. T. T. Tuyen, T. Ono, H. Miyashita, Y. Suzuki, H. Mimura, and M. Esashi, *J. Vac. Sci. Technol. B* **21**, 1705 (2003).

⁷W. I. Milne, K. B. K. Teo, M. Chhowalla, G. A. J. Amaratunga, D. Pribat, P. Legagneux, G. Pirio, Vu Thien Bind, and V. Semet, *J. Appl. Phys.* **94**, 487 (2003).

⁸W. A. D. Heer, A. Chätelain, and D. Ugarte, *Science* **270**, 1179 (1995).

⁹P. G. Collins and A. Zettl, *Phys. Rev. B* **55**, 9391 (1997).

¹⁰K. B. K. Teo, M. Chhowalla, G. A. Amaratunga, W. I. Milne, G. Pirio, P. Legagneux, D. Pribat, and D. G. Hasko, *Appl. Phys. Lett.* **80**, 2011 (2002).

¹¹G. C. Kokkorakis, A. Modinos, and J. P. Xanthakis, *J. Appl. Phys.* **91**, 4580 (2002).

¹²G. C. Kokkorakis, J. A. Roumeliotis, and J. P. Xanthakis, *J. Appl. Phys.* **95**, 1468 (2004).

¹³X. Zheng, G. H. Chen, Z. B. Li, S. Z. Deng, and N. S. Xu, *Phys. Rev. Lett.* **92**, 106803 (2004).

¹⁴A. Buldum and J. P. Lu, *Phys. Rev. Lett.* **91**, 236801 (2003).

¹⁵L. Nilsson, O. Groening, C. Emmenegger, O. Kuettel, E. Schaller, L. Schlapbach, H. Kind, J.-M. Bonard, and K. Kern, *Appl. Phys. Lett.* **76**, 2071 (2000).

¹⁶X. Q. Wang, Y. B. Xu, H. L. Ge, and M. Wang, *Diamond Relat. Mater.* **15**, 1565 (2006).

¹⁷M. Wang, Z. H. Li, X. F. Shang, X. Q. Wang, and Y. B. Xu, *J. Appl. Phys.* **98**, 014315 (2005).

¹⁸A. A. G. Driskill-Smith, D. G. Hasko, and H. Ahmed, *Appl. Phys. Lett.* **75**, 2845 (1999).

¹⁹J. C. She, S. Z. Deng, N. S. Xu, R. H. Yao, and J. Chen, *Appl. Phys. Lett.* **88**, 013112 (2006).

²⁰Y. C. Lan, C. T. Lee, Y. Hu, S. H. Chen, C. C. Lee, B. Y. Tsui, and T. L. Lin, *J. Vac. Sci. Technol. B* **22**, 1244 (2004).

²¹Y. M. Wong, W. P. Kang, J. L. Davidson, B. K. Choi, W. Hofmeister, and J. H. Huang, *Diamond Relat. Mater.* **14**, 2069 (2005).

²²D. Nicolaescu, V. Filip, S. Kanemaru, and J. Itoh, *J. Vac. Sci. Technol. B* **21**, 366 (2003).

²³A. A. G. Driskill-Smith, D. G. Hasko, and H. Ahmed, *J. Vac. Sci. Technol. B* **18**, 3481 (2000).

²⁴D. Nicolaescu, *J. Vac. Sci. Technol. B* **13**, 531 (1995).

²⁵D. Nicolaescu, M. Nagao, V. Filip, S. Kanemaru, and J. Itoh, *Jpn. J. Appl. Phys., Part 1* **44**, 3854 (2005).